

Gating Operation of Transport Current in Graphene Nanoribbon Fabricated by Helium Ion Microscope

Shu Nakaharai¹, Tomohiko Iijima², Shinichi Ogawa², Hisao Miyazaki³, Songlin Li³, Kazuhito Tsukagoshi³, Shintaro Sato¹ and Naoki Yokoyama¹

¹Green Nanoelectronics Center, AIST, ²Innovation Center for Advanced Nanodevices, AIST

16-1 Onogawa, Tsukuba, Ibaraki 305-8569, Japan

Phone: +81-29-849-1483, E-mail: shu-nakaharai@aist.go.jp

³NIMS-MANA

1-1 Namiki, Tsukuba, Ibaraki 305-0044, Japan

1. Introduction

Graphene, a two-dimensional sheet of carbon atoms[1], is a promising channel material for future transistors because of its extremely high carrier mobility as high as $200,000 \text{ cm}^2/\text{Vs}$ for both electrons and holes[2,3]. Such high mobility, along with the immunity to short channel effect due to atomically thin body[4], enables super high-speed and ultra low-energy consumption LSIs. For the application of graphene to electronics, however, there is a serious bottleneck, that is, a difficulty in generating an energy band gap. Graphene nanoribbon (GNR) is considered as one of the solutions for this issue, but it requires an extremely high spatial resolution better than 10 nm, which is quite difficult for the current lithography technique. Chemically derived[5], or CNT unzipped[6] GNRs are possible alternatives, but these bottom-up processes are not industrially feasible for device integration.

A Helium Ion Microscope (HeIM), which has recently been commercialized by CARL ZEISS, overcomes this issue due to its sub-nanometer size ion beam. In fact, Lemme and Bell[7,8] found that graphene can be etched directly by the He ion beam without resists, and demonstrated sub-10-nm size graphene nanoribbon fabrication. Their pioneering work opened a door to a fully top-down fabrication of graphene nano devices, but, to our knowledge, no one has yet succeeded in on-off gating of the transport current in HeIM-fabricated GNRs, possibly due to re-deposition of etched materials.

In this work, for the first time, we realized the on-off gating of current through a GNR fabricated by He ion beam etching, which has been realized by careful tuning of the etching conditions.

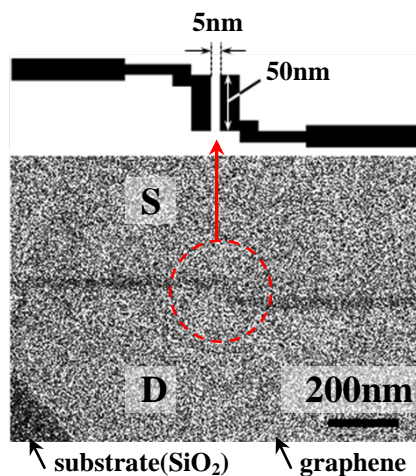


Fig.1. Helium ion micrograph of a GNR device. In the dark region, graphene is removed by the helium ion beam. A GNR with 5 nm width and 50 nm length is fabricated between source and drain regions as illustrated.

2. Experimental Results and Discussion

Single layer graphene flakes were mechanically exfoliated from a crystal of HOPG using adhesive tape, and then deposited on a silicon wafer with a 300-nm-thick surface thermal oxide layer. The number of graphene layers was identified by sight with an optical microscope. On the obtained graphene flakes, source and drain contacts were patterned by electron-beam lithography, and a Ti/Au (5/30 nm) layer were formed by thermal evaporation and lifting off. Drain current was measured with the back gate bias sweeping in order to detect the Dirac point ($V_{BG} = 2.5 \text{ V}$) and to estimate the contact resistance ($\sim 500 \Omega$).

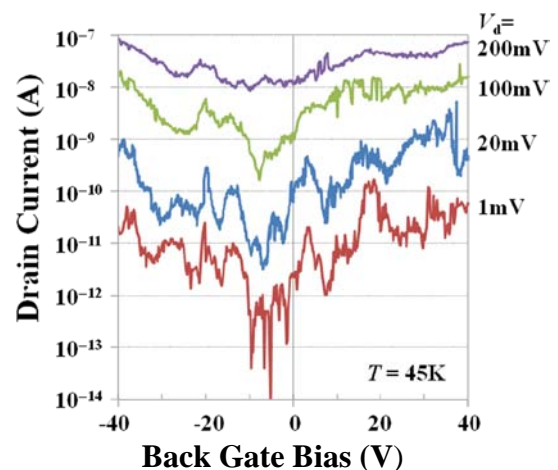


Fig. 2. Back gate bias (V_{BG}) dependence of drain current (I_d) at different drain biases (V_d) at $T = 45 \text{ K}$.

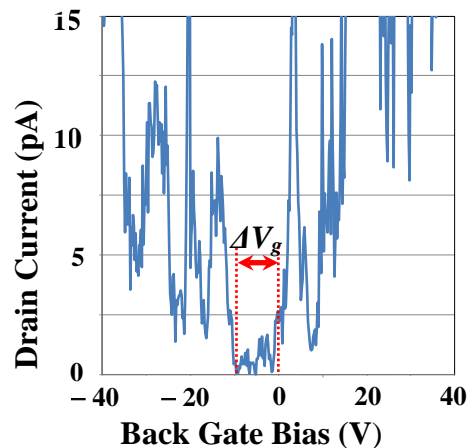


Fig. 3. A magnified view of I_d - V_{BG} curve of $V_d = 1 \text{ mV}$ plotted in linear scale. A ΔV_g range between -10 V and 0 V corresponds to the transport gap.

A graphene nanoribbon with 5 nm width and 50 nm length was fabricated using the HeIM as shown in Fig. 1. Here, source (S) and drain (D) regions are separated by rectangular dark regions where graphene was removed by He ion beam etching. And in the middle of this separating lines, a GNR was fabricated between the source and drain regions, as highlighted by a circle with a red broken line. After etching, the drain current was changed from 1.6×10^{-5} A to 2.8×10^{-8} A at $V_d = 50$ mV, $V_{BG} = 0$ V, at room temperature.

Figure 2 represents the back gate bias dependence of the drain current at different drain biases at $T = 45$ K. As shown in the figure, the drain current is strongly suppressed between -10 V and 0 V, and apart from this region, the drain current increases exponentially. Most of the spike-like peaks are reproduced by multiple measurements, suggesting that these signals reflect the resonant conduction through localizing sites which are proper to each GNR. The on-off ratio at $V_d = 1$ mV is estimated at about two orders of magnitude, and this ratio decreases as the drain bias increases, and almost disappears if $V_d > \sim 200$ mV. The back gate bias range, ΔV_g , that corresponds to the transport gap, is estimated to be about 10 V by determining voltage values at which the curve shows an inflection point[9], as shown in Fig. 3. This values is close to that in a preceding GNR experiment[10]. According to the reference[10], the energy scale for the transport gap, δ_T , should be evaluated to be ~ 200 meV[11]. It should be noted that the obtained energy scale for the transport gap is also close to an empirical band gap formula by Li *et al.*[5], $E_g = 0.8/w$, where w is the ribbon width in nanometer unit and E_g is the band gap in electron volt unit.

On the other hand, the temperature dependence of the off state properties of the current or conductivity should give the information on the energy scale corresponding to the thermally activated carrier transport. Figure 4 is the drain current of the on state (red) and the off state (blue) at $T = 45$ K. Differential conductance, which is defined as $G = dI_d/dV_d$, is derived from these curves and plotted in the inset as a function of V_d . The minimum value of the conductance, G_{\min} , is defined by the value of G at $V_d = 0$ V, and its temperature dependence is plotted in Fig. 5 (a) as a function of $1/T$. The temperature dependence of G_{\min} shows the feature of the thermally activated transport,

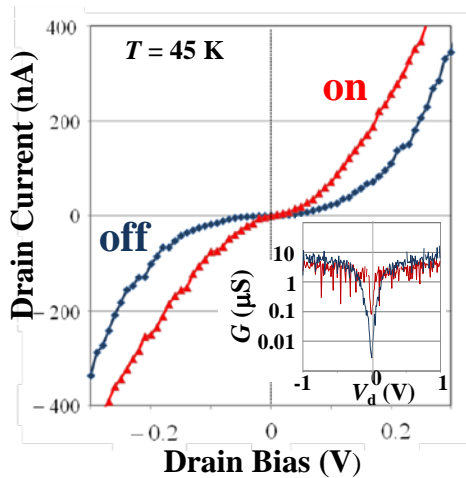


Fig. 4. Drain bias dependence of drain current of on (red) and off (blue) configurations at $T = 45$ K. In the off state curve, there is a flat region around zero bias. The inset shows the differential conductance of on (red) and off (blue) states. The off state exhibits a steep conduction drop in the four orders of the magnitude at $V_d = 0$ V.

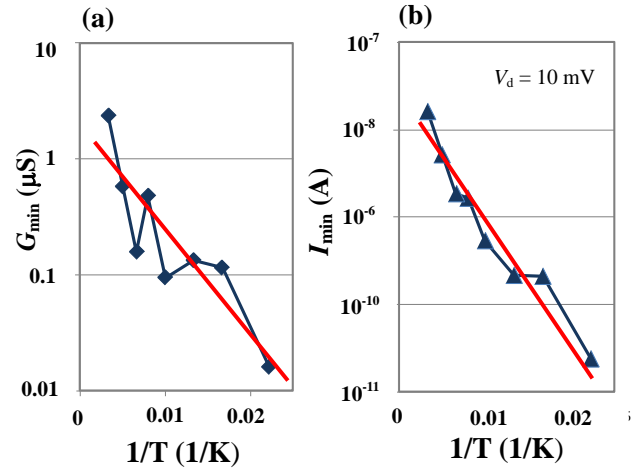


Fig. 5. Arrhenius plots of the minimum conductance, G_{\min} (a) and the minimum current, I_{\min} (b). Red lines are the fittings to extract the activation energy, E_a , according to eq (1), resulting in 48 meV (a) and 56 meV (b).

$$G_{\min} \propto \exp(-E_a/2k_B T), \quad (1)$$

where E_a is the activation energy and k_B is the Boltzmann's constant. From the fitting shown by a red line in Fig. 5(a), the activation energy is evaluated to be 48 meV. Similarly, the activation energy is also estimated by the temperature dependence of the minimum current of I_d at $V_d = 10$ mV, as denoted by I_{\min} , at $V_d = 10$ mV, as shown in Fig. 5(b), yielding a slightly larger value of 56 meV. The obtained activation energy, E_a , which is much smaller than the transport gap energy scale, $\delta_T \sim 200$ meV, implies that the transport cannot be explained by the thermally activated carriers going over the potential barrier caused by the energy gap. Instead, one possible explanation is that the current flows via localization levels in the transport gap, as previously discussed for lithographically fabricated GNRs[10]. But still, the origin of the carrier transport through GNRs is under discussion.

3. Summary

A GNR is fabricated by He ion beam etching using the HeIM, and, for the first time, its on-off operation of the transport current has been realized at cryogenic temperatures. The transport gap energy scale is evaluated to be 200 meV, which is much larger than the activation energy of about 50 meV, suggesting the transport by hopping through localization sites on GNRs.

Acknowledgements

This research is granted by the Japan Society for the Promotion of Science (JSPS) through the "Funding Program for World-Leading Innovative R&D on Science and Technology (FIRST Program)," initiated by the Council for Science and Technology Policy (CSTP).

References

- [1] K. Novoselov, *et al.* Science **306**, 666 (2004).
- [2] S. Morozov *et al.*, PRL **100**, 016602 (2008).
- [3] K. Bolotin, *et al.*, Solid State Comm. **146**, 351 (2008).
- [4] F. Schwierz, Nature Nano., **5**, 487 (2010).
- [5] X. Li, *et al.*, Science **319**, 1229 (2008).
- [6] D. Kosynkin, *et al.*, Nature **458**, 872 (2009).
- [7] M. Lemme, *et al.*, ACS Nano **3**, 2674 (2009).
- [8] D. Bell, *et al.*, Nanotechnology **20**, 455301 (2009).
- [9] E. Mucciolo, *et al.*, PRB **79**, 075407 (2009).
- [10] M. Han, *et al.*, PRL **104**, 056801 (2010).
- [11] A. Castro Neto, *et al.*, Rev. of Mod. Phys. **81**, 109 (2009).